Research Square

Preprints are preliminary reports that have not undergone peer review.
They should not be considered conclusive, used to inform clinical practice,
or referenced by the media as validated information.

Growth-related, antifungal and metal-binding activities of Penicillium janthinellum Z1-1031

Meng-Yue Zhang
Shenyang Pharmaceutical University
Ying-Ying Wu
Shenyang Pharmaceutical University
Zheng-Xu Sun
Shenyang Pharmaceutical University
Si-Yu Han
Shenyang Pharmaceutical University
Jun Xie
Shenyang Pharmaceutical University
Ming Cai
County Economic Development Service Center of Huanren Manchu Autonomous County
Ping Cao
County Economic Development Service Center of Huanren Manchu Autonomous County
Yan-Jun Hao
County Economic Development Service Center of Huanren Manchu Autonomous County
Yi-Xuan Zhang
zhangyxzsh@163.com

Shenyang Pharmaceutical University

Research Article

Keywords: Panax notoginseng, Penicillium janthinellum, brefeldin A, antifungal activity, metal biosorption

Posted Date: September 15th, 2026

DOI: https://doi.org/10.21203/rs.3.rs-10861855/v1

License: This work is licensed under a Creative Commons Attribution 4.0 International License.
Read Full License

Additional Declarations: No competing interests reported.

Abstract

Plant-associated fungi can influence plant performance while also interacting with phytopathogens and environmental contaminants. In this study, *Penicillium janthinellum* Z1-1031, a previously characterized fungus associated with *Panax notoginseng*, was investigated for its plant-associated, antifungal, and metal-interacting properties. Brefeldin A (BFA) was identified as a major secondary metabolite of Z1-1031. Purified BFA inhibited the growth of *Fusarium solani in vitro* in a concentration-dependent manner, while low BFA concentrations caused little detectable membrane damage in *P. notoginseng* root-tip cells. Following soil inoculation, viable Z1-1031 could be recovered from the rhizosphere for up to 56 days, and BFA was detected in rhizosphere soil 49 days after inoculation. In greenhouse experiments, Z1-1031 treatment increased the survival and biomass of *P. notoginseng* and transiently increased ginsenoside Rg1 content during the early cultivation period. Activities of peroxidase, superoxide dismutase, and catalase in roots were also elevated following Z1-1031 treatment. In addition, Z1-1031 showed *in vitro* biosorption capacity toward Cd, As, Cu, and Pb and transformed As(V) to As(III) in liquid culture. Z1-1031-treated cultivation soil showed lower measured concentrations of As, Cd, Pb, and Cu than the corresponding blank controls at one and four months. Collectively, these results characterize Z1-1031 as a multifunctional plant-associated fungus displaying plant-growth-related, *in vitro* antifungal, antioxidant-response-associated, and metal-interacting traits. The findings provide a basis for further evaluation of Z1-1031 in *P. notoginseng* cultivation, while its efficacy against root rot in planta, the environmental consequences of arsenic transformation, and the safety and fate of BFA require further investigation.

Key points

- Z1-1031 was associated with greater Panax notoginseng growth and root biomass.
- Purified BFA showed concentration-dependent inhibition of Fusarium solani in vitro.
- Z1-1031 showed metal biosorption and transformed As(V) to As(III) in liquid culture.

Introduction

Panax notoginseng (Burk.) F.H. Chen is an important traditional Chinese medicinal plant widely used for the treatment of cardiovascular diseases and blood circulation disorders. Its roots contain various pharmacologically active constituents, particularly ginsenosides, which exhibit anti-inflammatory, hemostatic, and cardioprotective activities (Dong et al. 2003; Sun et al. 2005). However, the sustainable cultivation of *P. notoginseng* is constrained by soil-borne diseases and deterioration of the soil environment. Root rot is among the most destructive diseases affecting *P. notoginseng* production and can substantially reduce plant survival, yield, and medicinal quality (Ma et al. 2013; Tan et al. 2017). Several fungal pathogens have been associated with root rot, including *Fusarium solani*, *Fusarium oxysporum*, *Cylindrocarpon destructans*, and *Alternaria panax* (Miao et al. 2006; Wang et al. 2015). Recent studies further demonstrate that changes in root-associated microbial communities are closely

associated with the occurrence and development of root rot in *P. notoginseng* (Chen et al. 2024; Liu et al. 2025a).

Plant-associated microorganisms are increasingly recognized as important contributors to plant growth and adaptation to environmental stresses. Rhizosphere and endophytic microorganisms can influence plant performance through nutrient mobilization, production of bioactive metabolites, antagonism toward phytopathogens, and modulation of host physiological responses (Avis et al. 2008; Berg et al. 2020; Compant et al. 2021; Mishra et al. 2017; Trivedi et al. 2020). Fungi represent an important component of these plant-associated microbial communities and can produce diverse secondary metabolites with biological activities relevant to plant–microbe interactions (Akram et al. 2023; Qin et al. 2024). Such metabolites may directly affect competing microorganisms or influence physiological responses of the host plant, providing a potential link between microbial persistence in the rhizosphere and effects on plant performance.

Species of the genus *Penicillium* are widely distributed in soil and rhizosphere environments, and several strains exhibit plant growth-promoting or antagonistic activities. For example, mycelial extracts of *Penicillium chrysogenum* have been reported to induce disease resistance in crop plants and suppress phytopathogens (Thuerig et al. 2006), while *Penicillium simplicissimum* GP17-2 induced systemic resistance in *Arabidopsis thaliana* (Hossain et al. 2007). Microbial interactions with plants are also frequently accompanied by changes in antioxidant defense. Peroxidase (POD), superoxide dismutase (SOD), and catalase (CAT) contribute to cellular redox homeostasis under biotic and abiotic stress by regulating reactive oxygen species (Wu et al. 2014). Microbial elicitation has additionally been associated with changes in secondary metabolism in medicinal plants (Prasad et al. 2022; Razzaq et al. 2025). These observations suggest that characterization of rhizosphere fungi should consider not only direct antagonism toward pathogens but also their associations with host growth, physiological responses, and accumulation of medicinally relevant metabolites.

In addition to soil-borne disease, metal contamination represents an important consideration in the cultivation and quality control of medicinal plants. *P. notoginseng* can accumulate elements such as arsenic (As), cadmium (Cd), copper (Cu), and lead (Pb), potentially affecting the safety and quality of medicinal materials (Yan et al. 2011). Recent evidence further indicates that Cd exposure can alter both the growth and saponin accumulation of *P. notoginseng* as well as its rhizosphere microbial community (Liu et al. 2025b). Microorganisms can interact with metals through biosorption, bioaccumulation, complexation, and redox transformation, thereby altering their distribution and chemical speciation in soil environments (Gadd 2010; Narendrula-Kotha and Nkongolo 2017). Several *Penicillium* species possess metal-binding or transformation capacities. *P. simplicissimum*, for example, exhibits tolerance to Ni and Co and can adsorb Cd, Pb, and Zn (Valix et al. 2001; Fan et al. 2008), whereas *P. janthinellum* has been implicated in arsenic transformation (Su et al. 2011). These properties raise the possibility that plant-associated *Penicillium* strains may simultaneously interact with plants, phytopathogens, and metal contaminants in the rhizosphere.

Despite these observations, the multiple functional traits of *P. notoginseng*-associated fungi have not been sufficiently characterized within a single experimental system. In particular, it remains unclear whether an individual plant-associated fungal strain can simultaneously display plant-growth-related and antifungal traits together with measurable effects on host physiological responses and interactions with environmental metals. Establishing these phenotypes separately is important before causal relationships among them or their practical agricultural applications can be defined.

In the present study, the previously characterized *P. notoginseng*-associated fungus *P. janthinellum* Z1-1031 was used, and brefeldin A (BFA) was identified as a major secondary metabolite produced by this strain. We characterized the antifungal activity and plant-cell effects of BFA, monitored the persistence of Z1-1031 and the occurrence of BFA in rhizosphere soil after inoculation, and evaluated the effects of fungal or BFA treatment on *P. notoginseng* growth, ginsenoside accumulation, and antioxidant enzyme activities. In parallel, the metal biosorption capacity and arsenic transformation activity of Z1-1031 were examined, together with changes in As, Cd, Pb, and Cu concentrations in cultivation soil following fungal inoculation. Here, we aimed to characterize multiple phenotypes of Z1-1031 under in vitro and greenhouse conditions. The overarching question was whether a single *P. notoginseng*-associated fungus could display experimentally distinguishable plant-growth-related, antifungal, and metal-interacting traits within the same experimental framework. These phenotypes were evaluated as distinct outcomes rather than as components of a presumed common mechanism

Materials and Methods

Fungal strain and taxonomic assignment

Strain Z1-1031 was previously isolated from the surface-sterilized root of a healthy *Panax notoginseng* plant collected in Wenshan, Yunnan Province, China, and was maintained in our laboratory culture collection. The strain was originally reported as *Penicillium* sp. SYP-ZL1031, and its ITS sequence was deposited in GenBank under accession number KU360251 (Xie et al. 2017). Subsequent characterization assigned this strain to *Penicillium janthinellum* (Xie et al. 2018).

Fermentation of strain Z1-1031 and isolation of brefeldin A

Solid-state fermentation of strain Z1-1031 was performed in 100 250-mL Erlenmeyer flasks containing rice medium. After inoculation, the cultures were incubated statically at 28°C for 30 days. The fermented material was extracted with ethyl acetate overnight and sonicated for 1 h. Extraction was repeated three to four times, and the combined extracts were concentrated under reduced pressure. The crude extract was dissolved in 90% methanol–water and partitioned with cyclohexane. The methanolic fraction was subsequently subjected to silica-gel column chromatography. The fraction eluted with methanol–H_2O was further separated using an ODS column to obtain 15 subfractions (B1–B15). Subfraction B4 was

purified using Sephadex LH-20 followed by semi-preparative HPLC to yield colorless needle-shaped crystals.

The purified compound was characterized by ^{1}H NMR, ^{13}C NMR, and high-resolution electrospray ionization mass spectrometry (HR-ESI-MS). Its spectroscopic data were compared with previously reported data for brefeldin A (BFA). Detailed ^{1}H and ^{13}C NMR data are provided in Table S1.

In vitro antifungal activity of BFA against Fusarium solani

Fusarium solani was cultured on PDA at 28°C for 7 days. Spores were harvested in sterile water, and the suspension was adjusted to OD_{600} = 0.2. One milliliter of the spore suspension was mixed with 24 mL potato dextrose broth, and 198 µL of this mixture was dispensed into each well of a 96-well microplate. BFA solution (2 µL) was added to obtain final concentrations of 20, 200, and 1000 µg mL^{-1}. Untreated cultures served as the negative control, whereas G418 and imazalil, each at a final concentration of 2 µg mL^{-1}, were used as positive controls. The plates were incubated at 28°C for 24 h, after which fungal growth was quantified by measuring OD_{600} using a microplate reader.

Effects of BFA on P. notoginseng root-tip cells

Fibrous root tips of *P. notoginseng* were collected and washed with sterile water. Root tips were exposed to BFA at concentrations of 0, 20, 50, 200, 1000, and 5000 µg mL^{-1} for 24 h under a 12-h light/12-h dark photoperiod, with temperatures of 25°C during the light period and 20°C during the dark period. Following treatment, root tips were stained with propidium iodide (PI; 5 µg mL^{-1}) and examined using a Leica DM2000 fluorescence microscope (Leica, Germany) with excitation at 488 nm and emission at 630 nm.

PI fluorescence was quantified using ImageJ. For each image, the red fluorescence-positive area was measured and expressed relative to the total analyzed root-tip area. Three independent biological replicates were analyzed for each treatment.

Construction of the EGFP-labeled strain and assessment of persistence in rhizosphere soil

The absence of the *egfp* gene in wild-type Z1-1031 was first confirmed by PCR. The sensitivity of Z1-1031 to hygromycin B was evaluated, and 500 µg mL^{-1} hygromycin B was used for selection of transformants. Plasmid pTFCM, carrying *egfp* and a hygromycin-resistance marker, was introduced into Z1-1031 by *Agrobacterium tumefaciens*-mediated transformation using strain AGL-1. Following co-cultivation at 26°C for 48 h, transformants were selected on PDA containing 500 µg mL^{-1} hygromycin B. EGFP fluorescence of the resulting strain, Z1-1031-egfp, was examined by fluorescence microscopy. The plasmid pTFCM and *A. tumefaciens* AGL-1 were obtained as described in the original study records.

For the soil-persistence experiment, a Z1-1031-egfp spore suspension was prepared at 1×10^5 CFU mL^{-1} in sterile deionized water. Each plant received 50 mL of the suspension applied to the rhizosphere soil. A total of 140 plants were treated and maintained in a greenhouse at 25°C with watering every 2 days. Rhizosphere soil was sampled at 0, 1, 3, 6, 10, 15, 21, 28, 35, 42, 49, and 56 days after inoculation. Z1-1031-egfp was recovered on selective medium, and recoverable fungal populations were expressed as CFU per gram of soil. CFU enumeration was used to assess the persistence and recoverability of viable Z1-1031 propagules from rhizosphere soil and did not assess physical attachment to root surfaces or endophytic colonization of root tissues.

Detection of BFA in rhizosphere soil

To determine whether BFA was detectable in rhizosphere soil following fungal inoculation, Z1-1031 spore suspensions were applied to the rhizosphere of *P. notoginseng*. Soil samples were collected at 7-day intervals for up to 49 days. Soil extracts were analyzed by liquid chromatography–electrospray ionization quadrupole time-of-flight mass spectrometry (LC-ESI-QTOF-MS) in positive-ion mode.

BFA was identified by comparison of retention time and the characteristic ion signal with those of an authentic BFA standard. Uninoculated soil treated with sterile water was analyzed as a control.

Greenhouse treatments and measurement of plant growth

For evaluation of plant responses, strain Z1-1031 was applied to the rhizosphere soil as described above. BFA was separately applied to the rhizosphere soil at 10 μg mL^{-1}, whereas sterile deionized water served as the blank control. Plants were maintained in a greenhouse at 25°C and watered every 2 days. Each treatment comprised three independent plots. At each sampling time, at least ten plants were randomly selected from each plot for measurement of plant growth traits. Measurements obtained from individual plants within each plot were averaged to generate one plot-level value, and the plot was treated as the experimental unit. The same plots were followed throughout the experiment, whereas different plants were sampled at one and four months because root fresh- and dry-weight measurements required destructive sampling. Plant survival and growth were assessed after one and four months. Measurements included plant height, leaf number, leaf fresh weight, shoot fresh weight, root fresh weight, and root dry weight.

Determination of saponins and antioxidant enzyme activities

Saponins were extracted from P. notoginseng roots according to the procedure described in the Chinese Pharmacopoeia (2025 edition) and analyzed using an Agilent 1260 HPLC system equipped with a diode-array detector. Separation was performed on an Agilent XDB-C18 column (4.6 × 150 mm, 2.7 μm) using acetonitrile and water as the mobile phases. The acetonitrile gradient was 20–22% from 0 to 20 min, 22–

46% from 20 to 45 min, 46–55% from 45 to 50 min, and 55–90% from 50 to 53 min. The flow rate was 0.5 mL min^{-1}, the detection wavelength was 203 nm, and the column temperature was maintained at 30°C. Notoginsenoside R1 and ginsenosides Rg1, Re, Rb1, and Rd were quantified using an external-standard method.

Activities of peroxidase (POD), superoxide dismutase (SOD), and catalase (CAT) in root samples were measured using commercial assay kits (Keming Biotechnology, Suzhou, China) according to the manufacturer's instructions.

Arsenic transformation assay

To examine arsenic transformation by Z1-1031, 100 µL of a fungal spore suspension (1×10^7 CFU mL^{-1}) was inoculated into 12 mL of shaking potato–glucose–peptone medium containing 50 mg L^{-1} As(V), supplied as $Na_2HAsO_4 \cdot 7H_2O$. This corresponded to a nominal initial As(V) amount of 600 µg per culture. Culture samples were collected after 3, 5, and 10 days.

Total inorganic arsenic and As(III) in the culture broth and fungal biomass were determined using an atomic fluorescence spectrometer coupled to a hydride-generation system (Aurora, Italy). As(V) was determined as the difference between total inorganic arsenic and As(III). Arsenic amounts recovered from the broth and fungal biomass are reported as µg per culture in Table 3.

Metal biosorption assay

The biosorption of Cd(II), As(III), Cu(II), and Pb(II) by strain Z1-1031 was evaluated in liquid fungal cultures. Each metal was supplied separately at a final concentration of 50 mg L^{-1} using $CdCl_2 \cdot 2.5H_2O$, As_2O_3, $CuSO_4$, or $Pb(NO_3)_2$, respectively. Uninoculated medium containing the corresponding metal served as the abiotic control, and three independent cultures were prepared for each treatment. Cultures were incubated under shaking conditions for 48 h.

After incubation, the cultures were centrifuged, and 3 mL of the resulting supernatant was mixed with 3 mL concentrated HNO_3 and diluted to a final volume of 45 mL with deionized water. Residual metal concentrations in the supernatants were determined by inductively coupled plasma mass spectrometry (ICP-MS) by an external analytical service. Fungal biomass was collected and its dry weight was determined for normalization of metal uptake. Biosorption capacity was expressed as mmol kg^{-1} dry biomass and calculated from the decrease in dissolved metal concentration using $q = (C_0\text{-}C_e)V/m$, where C_0 and C_e are the initial and residual metal concentrations, respectively, V is the culture volume, and m is the fungal dry biomass.

Determination of metal concentrations in cultivation soil

To examine changes in soil metal concentrations following fungal treatment, strain Z1-1031 was applied to *P. notoginseng* cultivation soil as described above, while soil receiving sterile deionized water served as the blank control. Rhizosphere soil samples were collected from three independent plots per treatment after one and four months. Soil samples were air-dried, finely ground, and prepared for metal analysis following the procedure described by Ou et al. (2016). Briefly, 0.25 g of each soil sample was digested with 10 mL HCl and 0.5 mL $HClO_4$ and subsequently diluted with 10 mL distilled water. Cd, Pb, and Cu were quantified by atomic absorption spectrometry, whereas As was determined by hydride-generation atomic fluorescence spectrometry. Metal analyses were performed by an external analytical laboratory, and concentrations are expressed as mg kg^{-1} dry soil. Three independent plot-derived soil samples were analyzed for each treatment and sampling time.

Statistical analysis

Data are presented as mean ± standard deviation (SD), unless otherwise indicated. For plant experiments, each treatment consisted of three independent plots. At each sampling time, measurements obtained from at least ten plants within each plot were averaged to generate one plot-level value, and the plot was treated as the experimental unit (n = 3 plots per treatment). The same plots were followed at one and four months, although different plants were sampled at the two time points for destructive measurements.

For variables measured at both one and four months, treatment, time, and the treatment × time interaction were analyzed using a linear mixed-effects model, with treatment and time as fixed effects and plot nested within treatment as a random effect. When significant effects were detected, pairwise comparisons among treatments at each sampling time were performed with Tukey adjustment for multiple comparisons. Single-factor experiments were analyzed by one-way analysis of variance (ANOVA) followed by Tukey's multiple-comparison test when appropriate. Percentage outcomes, including plant survival and PI-positive area, were analyzed on the original percentage scale at the corresponding plot or biological-replicate level. Model residuals were examined for approximate normality and homogeneity of variance. Differences were considered statistically significant at $P < 0.05$.

The CFU time-course data were used descriptively to assess persistence of Z1-1031 in rhizosphere soil and were not subjected to inferential comparisons among sampling times.

Results

Taxonomic and morphological characteristics of strain Z1-1031

Strain Z1-1031 was previously reported as a *Panax notoginseng*-associated *Penicillium* strain, with its ITS sequence deposited in GenBank under accession number KU360251 (Xie et al. 2017). Subsequent characterization assigned the strain to *P. janthinellum* (Xie et al. 2018).

On potato dextrose agar (PDA), strain Z1-1031 formed nearly circular colonies with a dark-green surface, loose floccose mycelia, and a yellow reverse (Fig. 1A). Microscopic examination showed relatively long and robust conidiophores arising from aerial hyphae, with smooth walls and septate structures (Fig. 1B). These morphological characteristics were consistent with those previously described for *P. janthinellum* (Matsukuma et al. 1994). Based on the previously deposited ITS sequence, earlier taxonomic characterization, and the morphological characteristics observed here, the strain is referred to as *P. janthinellum* Z1-1031 throughout this study.

Isolation and structural identification of brefeldin A

To characterize the major secondary metabolite produced by strain Z1-1031, the fermented material was extracted and subjected to chromatographic separation. A major compound was purified and characterized by ^{1}H NMR, ^{13}C NMR, and HR-ESI-MS. Its spectroscopic characteristics were consistent with published data for brefeldin A (BFA) (Wang et al. 2007). The chemical structure of the identified compound is shown in Fig. 1C, and detailed NMR data are provided in Table S1. Thus, BFA was identified as a major metabolite produced by *P. janthinellum* Z1-1031 under the culture conditions used in this study.

In vitro antifungal activity of brefeldin A against Fusarium solani

The antifungal activity of purified BFA was evaluated against *F. solani*, a fungal pathogen associated with root rot of *P. notoginseng*. BFA inhibited the growth of *F. solani* in a concentration-dependent manner (Fig. 2). Compared with the untreated control, BFA at 20 μg mL^{-1} reduced fungal growth by approximately 15.5% ($P < 0.05$). The inhibition increased to approximately 47.1% and 71.8% at 200 and 1000 μg mL^{-1}, respectively ($P < 0.001$), demonstrating a clear concentration-dependent antifungal effect (Fig. 2).

The activity of BFA was also compared with G418 and imazalil at 2 μg mL^{-1}. Both positive controls inhibited *F. solani* growth, while increasing concentrations of BFA produced progressively greater inhibition (Fig. 2). These results establish a concentration-dependent in vitro antifungal activity of BFA against *F. solani*.

Concentration-dependent effects of brefeldin A on *P. notoginseng* root-tip cells

The effects of BFA on *P. notoginseng* root-tip cells were evaluated by propidium iodide (PI) staining, in which increased red fluorescence indicates loss of plasma-membrane integrity. Root tips exposed to low BFA concentrations showed relatively weak PI fluorescence, whereas progressively stronger signals were observed at higher concentrations (Fig. 3).

At 20 and 50 μg mL^{-1} BFA, the PI-positive area accounted for approximately 8.6% and 9.7% of the analyzed root-tip area, respectively, whereas little PI-positive area was detected in the untreated control. The PI-positive proportion increased to approximately 20.5% at 200 μg mL^{-1} and further increased to approximately 33.8% and 56.2% at 1000 and 5000 μg mL^{-1}, respectively. These quantitative data,

together with the fluorescence images, demonstrate a concentration-dependent increase in membrane damage at higher BFA concentrations.

Persistence of strain Z1-1031 and detection of BFA in rhizosphere soil

Before construction of the EGFP-labeled strain, the sensitivity of wild-type Z1-1031 to hygromycin B was evaluated. Fungal growth was progressively inhibited with increasing hygromycin B concentrations and was markedly suppressed at 500–600 μg mL^{-1} (Fig. S1). Therefore, 500 μg mL^{-1} hygromycin B was used for transformant selection. An EGFP-labeled strain, Z1-1031-egfp, was subsequently constructed. The *egfp* gene was detected in the transformed strain but not in wild-type Z1-1031, and fluorescence microscopy showed a clear green fluorescent signal in Z1-1031-egfp (Fig. S2).

Following inoculation into *P. notoginseng* rhizosphere soil, viable Z1-1031-egfp could be recovered on PDA containing hygromycin B. The recoverable population decreased from approximately 1.0×10^5 CFU g^{-1} soil immediately after inoculation to approximately 1.0×10^4 CFU g^{-1} soil during the first 15 days. Thereafter, the population declined more slowly and remained detectable at approximately 10^3–10^4 CFU g^{-1} soil throughout the 56-day observation period (Fig. 4). These data show that viable Z1-1031 persisted in the rhizosphere soil for at least 56 days under the experimental conditions.

LC-ESI-QTOF-MS was subsequently used to determine whether BFA could be detected in rhizosphere soil following Z1-1031 inoculation. No corresponding BFA signal was detected in uninoculated control soil (Fig. S3B), whereas a peak matching the BFA reference standard was detected in Z1-1031-treated rhizosphere soil at day 49 (Fig. S3C). The detected ion at *m/z* 303.1584 and its retention time were consistent with those of the BFA standard (Fig. S3A). Thus, BFA was detectable in rhizosphere soil 49 days after inoculation with strain Z1-1031.

Effects of Z1-1031 and BFA on P. notoginseng growth

The effects of Z1-1031 and BFA on *P. notoginseng* performance were evaluated after one and four months of treatment (Tables 1 and 2). After one month, plant survival was 85.69%, 89.79%, and 87.14% in the control, Z1-1031, and BFA groups, respectively (Table 1). Several growth parameters were higher following Z1-1031 treatment. Leaf number increased from 20.33 ± 0.47 in the control to 27.67 ± 1.70 following Z1-1031 treatment. Leaf fresh weight increased from 2.13 ± 0.12 to 4.50 ± 0.40 g, shoot fresh weight from 3.93 ± 0.74 to 6.53 ± 0.37 g, root fresh weight from 9.46 ± 1.04 to 13.60 ± 0.43 g, and root dry weight from 2.37 ± 0.25 to 3.40 ± 0.20 g (Table 1). BFA treatment also increased some growth measurements during the first month, although the magnitude and statistical significance varied among parameters.

After four months, survival was 53.22 ± 3.07% in the Z1-1031 treatment compared with 39.26 ± 4.18% in the control (Table 2). Root fresh weight and dry weight in the Z1-1031 group reached 15.00 ± 0.81 and

5.27 ± 0.45 g, respectively, and were higher than the corresponding control values. In contrast, BFA treatment alone did not significantly alter survival or most growth parameters at four months.

Overall, Z1-1031 treatment was associated with sustained increases in several growth-related traits, particularly root biomass, whereas the effects observed with BFA alone were mainly evident during the earlier sampling period.

Effects of Z1-1031 and BFA on saponin contents

The concentrations of major saponins in *P. notoginseng* roots were determined after treatment with Z1-1031 or BFA (Fig. S4). After one month, ginsenoside Rg1 content reached 4.82% in the Z1-1031 group compared with 2.22% in the control, corresponding to an approximately 117% increase. This difference was significant at the first sampling point but was no longer evident after four months. Among the saponin outcomes shown in Fig. S4, the transient increase in Rg1 at one month was the only significant treatment-associated change. The combined content of the five measured saponins, comprising notoginsenoside R1 and ginsenosides Rg1, Re, Rb1, and Rd, did not differ significantly among treatments at either sampling time. Thus, the effect on saponin accumulation was most evident as a transient increase in Rg1 rather than a sustained increase in total measured saponins.

Effects of Z1-1031 and BFA on antioxidant enzyme activities

The activities of POD, SOD, and CAT were measured in *P. notoginseng* roots following treatment with Z1-1031 or BFA (Fig. 5). Z1-1031 treatment increased the activities of all three antioxidant enzymes relative to the untreated control. At one month, POD, SOD, and CAT activities were approximately 3.5-, 2.3-, and 3.1-fold those of the control, respectively. At four months, the corresponding activities remained approximately 3.2-, 2.4-, and 3.3-fold those of the control, respectively.

BFA treatment also increased POD, SOD, and CAT activities during the first month, to approximately 3.4-, 2.4-, and 3.3-fold those of the control, respectively. By four months, however, these responses had declined markedly, with POD, SOD, and CAT activities corresponding to approximately 1.1-, 1.3-, and 1.4-fold those of the control, respectively. These results show that both fungal inoculation and BFA exposure were associated with changes in root antioxidant enzyme activities, with the response to Z1-1031 being more persistent over the experimental period.

Arsenic transformation by strain Z1-1031

Arsenic speciation and recovery in the culture system were analyzed to characterize the interaction between Z1-1031 and inorganic arsenic (Table 3). In the uninoculated control, arsenic remained predominantly as As(V) throughout the incubation period.

In cultures containing Z1-1031, both As(V) and As(III) were detected in the broth. After five days, As(V) and As(III) accounted for approximately 52.6% and 47.4%, respectively, of dissolved arsenic. By day 10,

As(III) accounted for approximately 99.7% of the dissolved arsenic, indicating extensive reduction of As(V) to As(III).

Arsenic associated with fungal biomass was detected predominantly as As(V), whereas As(III) was not detected in the mycelial fraction. The measured total arsenic recovered from the broth and fungal biomass at the end of the experiment was approximately 27.4% lower than the initial amount.

These results demonstrate substantial transformation of As(V) to As(III) in the presence of Z1-1031. The decrease in recovered arsenic indicates an incomplete arsenic mass balance under the experimental conditions; the fate of the unrecovered fraction cannot be determined from the present data.

Metal biosorption by strain Z1-1031 and changes in soil metal concentrations

The biosorption capacity of Z1-1031 toward Cd, As, Cu, and Pb was evaluated under laboratory conditions (Fig. 6). Among the four metals tested, the highest biosorption capacity was observed for Cd (104 mmol kg^{-1} dry biomass), followed by As, Cu, and Pb, with Pb showing the lowest value (25.4 mmol kg^{-1}). These results demonstrate that Z1-1031 can bind multiple metals under the assay conditions, although the extent of biosorption differed among metals.

Changes in metal concentrations were monitored in P. notoginseng cultivation soil following Z1-1031 treatment (Fig. 7). After one month, the concentrations of As, Cd, Pb, and Cu in Z1-1031-treated soil were 25.33, 0.16, 32.68, and 12.01 mg kg^{-1}, respectively, compared with 49.31, 0.21, 42.40, and 15.17 mg kg^{-1} in the corresponding blank-control soil. After four months, the concentrations in Z1-1031-treated soil were 21.33 mg kg^{-1} As, 0.15 mg kg^{-1} Cd, 29.28 mg kg^{-1} Pb, and 11.38 mg kg^{-1} Cu and remained lower than those in the corresponding blank controls. These observations indicate that Z1-1031 treatment was associated with lower measured concentrations of several metals in cultivation soil.

Table 1
Growth responses of *Panax notoginseng* to strain Z1-1031 or brefeldin A after one month

Treatments	Survival rate (%)	Plant height (cm)	No. of leaves	Leaves FW(g)	Shoot FW (g)	Root FW (g)	Root DW (g)
Blank control	85.69 ± 1.03^{a}	24.78 ± 0.57^{a}	20.33 ± 0.47^{a}	2.13 ± 0.12^{a}	3.93 ± 0.74^{a}	9.46 ± 1.04^{a}	2.37 ± 0.25^{a}
Z1-1031	89.79 ± 2.63^{a}	26.84 ± 0.85^{a}	27.67 ± 1.70^{b}	4.50 ± 0.40^{b}	6.53 ± 0.37^{b}	13.60 ± 0.43^{b}	3.40 ± 0.20^{b}
BFA	87.14 ± 3.64^{a}	22.22 ± 1.60^{a}	25.33 ± 1.25^{b}	2.95 ± 0.48^{a}	4.46 ± 0.41^{a}	12.13 ± 0.66^{b}	3.03 ± 0.19^{b}

Values are presented as mean ± SD of three independent plots (n = 3). At least ten plants were randomly sampled within each plot at each sampling time, and individual plant measurements were averaged to

obtain one plot-level value. Because root fresh- and dry-weight measurements required destructive sampling, different individual plants were sampled at one and four months, while the same experimental plots were followed throughout the experiment. Treatment, time, and the treatment × time interaction were included as fixed effects in a linear mixed-effects model, with plot nested within treatment as a random effect. Different lowercase letters within a column indicate significant differences among treatments at the sampling time based on Tukey-adjusted pairwise comparisons ($P < 0.05$). FW, fresh weight; DW, dry weight.

Table 2
Growth responses of *Panax notoginseng* to strain Z1-1031 or brefeldin A after four months

Treatments	Survival rate (%)	Plant height (cm)	No. of leaf	Leaf FW(g)	Shoot FW (g)	Root FW (g)	Root DW (g)
Blank control	39.26 ± 4.18^{a}	35.67 ± 2.05^{a}	23.34 ± 2.36^{a}	4.83 ± 0.85^{a}	5.60 ± 0.43^{a}	12.25 ± 0.87^{a}	3.60 ± 0.43^{a}
Z1-1031	53.22 ± 3.07^{b}	37.00 ± 4.90^{a}	24.01 ± 2.16^{a}	6.23 ± 0.33^{a}	5.67 ± 0.47^{a}	15.00 ± 0.81^{b}	5.27 ± 0.45^{b}
BFA	38.10 ± 2.43^{a}	35.00 ± 4.24^{a}	24.67 ± 2.49^{a}	5.00 ± 0.82^{a}	6.57 ± 0.33^{a}	12.33 ± 0.47^{a}	4.07 ± 0.09^{a}

Values are presented as mean ± SD of three independent plots (n = 3). At least ten plants were randomly sampled within each plot at each sampling time, and individual plant measurements were averaged to obtain one plot-level value. Because root fresh- and dry-weight measurements required destructive sampling, different individual plants were sampled at one and four months, while the same experimental plots were followed throughout the experiment. Treatment, time, and the treatment × time interaction were included as fixed effects in a linear mixed-effects model, with plot nested within treatment as a random effect. Different lowercase letters within a column indicate significant differences among treatments at the sampling time based on Tukey-adjusted pairwise comparisons ($P < 0.05$). FW, fresh weight; DW, dry weight.

Table 3
Arsenic speciation and recovered arsenic amounts during incubation with strain Z1-1031

Samples	0 d	3 d		5 d		10 d	
	Arsenic amount (μg culture^{-1})	Arsenic amount (μg culture^{-1})		Arsenic amount (μg culture^{-1})		Arsenic amount (μg culture^{-1})	
Arsenic speciation	As(V) As(III)	As(V)	As(III)	As(V)	As(III)	As(V)	As(III)
Medium + As (uninoculated control)	600 ± 0.02 ND	598.24 ± 9.60	ND	590.24 ± 7.60	ND	590.33 ± 8.50	ND
Medium + As + Z1-1031 (broth)	599 ± 0.05 ND	402 ± 8.66	134.32 ± 9.67	259.78 ± 10.66	234.32 ± 19.67	1.20 ± 0.20	424.67 ± 11.47
Medium + As + Z1-1031 (fungal biomass)	NA NA	2.24 ± 0.09	ND	5.07 ± 0.19	ND	9.24 ± 0.23	ND

Quantifiable values are expressed as μg culture^{-1} and are presented as mean ± SD of three independent culture experiments (n = 3). NA, not applicable; ND, not detected. Values represent the recovered amounts of As(V) and As(III) in the culture broth or fungal biomass. For inoculated cultures, total recovered arsenic at each sampling time was calculated as the sum of As(V) and As(III) detected in the broth and fungal biomass.

Discussion

The present study investigated the previously characterized *Panax notoginseng*-associated fungus *Penicillium janthinellum* Z1-1031 and examined several biological activities relevant to plant performance and the rhizosphere environment. Inoculation with Z1-1031 was associated with improved plant survival and biomass, increased activities of antioxidant enzymes, and a transient increase in ginsenoside Rg1. The strain remained recoverable from rhizosphere soil for an extended period, and BFA was detected in the soil after fungal inoculation. Purified BFA inhibited *Fusarium solani* in vitro, whereas Z1-1031 also exhibited metal biosorption and arsenic transformation capacities under laboratory conditions. In cultivation soil, Z1-1031 inoculation was associated with lower measured concentrations of As, Cd, Pb, and Cu than the corresponding blank controls. Taken together, these observations indicate that Z1-1031 possesses multiple biological activities of potential relevance to *P. notoginseng* cultivation. Importantly, however, these activities represent distinct experimental observations and should not be interpreted as evidence for a single BFA-mediated mechanism or as proof of disease control or heavy-metal detoxification under cultivation conditions.

Growth responses of P. notoginseng to Z1-1031

Inoculation with Z1-1031 improved several growth-related parameters of *P. notoginseng*, including plant survival and root biomass. Such responses are consistent with the broader ability of plant-associated fungi to influence host growth and stress adaptation. Beneficial microorganisms may affect plant performance through nutrient mobilization, modification of the rhizosphere environment, production of bioactive metabolites, or changes in host physiological responses (Khan et al. 2008; Viterbo et al. 2010; Lugtenberg and Kamilova 2009). More broadly, plant-associated microbiota are increasingly regarded as functional components of plant performance rather than passive inhabitants of the rhizosphere (Berg et al. 2020; Trivedi et al. 2020).

Persistence in the rhizosphere is likely to be important for any sustained effect of an introduced microorganism. Z1-1031 remained recoverable from rhizosphere soil throughout the 56-day observation period, although its population declined rapidly during the early period before reaching a relatively stable level. Long-term persistence in the root-associated environment has been reported for several beneficial plant-associated fungi. Such persistence may be important for sustained effects on nutrient acquisition, host physiology, or stress responses (Baron and Rigobelo 2022; Compant et al. 2021; Qin et al. 2024). In the present study, however, recovery of Z1-1031 was assessed by CFU enumeration from rhizosphere soil. The data therefore demonstrate persistence of recoverable Z1-1031 populations in the rhizosphere, rather than direct colonization of root tissues or attachment to root surfaces.

The mechanisms responsible for the observed growth responses remain unresolved. Although BFA was detected in the rhizosphere following Z1-1031 inoculation, the present experiments do not demonstrate that BFA mediates plant growth promotion. Other fungal metabolites, changes in nutrient availability, or indirect effects on the rhizosphere environment could also contribute. Accordingly, the growth-promoting phenotype should presently be regarded as an effect associated with Z1-1031 inoculation rather than as a BFA-dependent response.

In vitro antifungal activity of BFA and its detection in the rhizosphere

A prominent finding of this study was the antifungal activity of BFA against *F. solani*. Purified BFA inhibited fungal growth in a concentration-dependent manner. At 20 μg mL^{-1}, fungal growth was already reduced, and substantially stronger inhibition was observed at 200 and 1000 μg mL^{-1}. These findings demonstrate concentration-dependent *in vitro* antifungal activity of BFA against this *P. notoginseng*-associated pathogen. Production of antimicrobial secondary metabolites is a well-established mechanism by which plant-associated fungi can antagonize competing or pathogenic microorganisms (Akram et al. 2023; Dasila et al. 2024; Wang et al. 2007; Wen et al. 2022).

The ecological relevance of this observation is strengthened by the detection of BFA in rhizosphere soil following inoculation with Z1-1031. Together, these experiments provide three related but distinct observations: Z1-1031 remained recoverable from rhizosphere soil, BFA was detected in the inoculated

rhizosphere, and purified BFA inhibited *F. solani in vitro*. These findings support BFA as one candidate metabolite contributing to the antagonistic potential of Z1-1031.

Nevertheless, the present evidence does not establish BFA as the causal mediator of root-rot suppression in planta. The concentration of BFA achieved at microsites within the rhizosphere was not quantified and therefore could not be directly related to the in vitro concentration–response data. More importantly, the current study did not include a plant infection experiment comparing pathogen-only and pathogen-plus-Z1-1031 treatments. Therefore, the data support the in vitro antifungal activity of BFA and its detection in rhizosphere soil, but not a conclusion that either BFA or Z1-1031 controls *F. solani* root rot in planta. This distinction is important because pathogen suppression in the rhizosphere can additionally depend on microbial competition, spatial interactions, metabolite stability, and interactions with resident microbial communities (Jayaraman et al. 2021; Rasool et al. 2025).

The PI-staining experiment further provides information on the response of *P. notoginseng* root-tip cells to BFA over the tested concentration range. Relatively limited PI-positive staining was observed at the lower concentrations, whereas membrane damage increased markedly at higher concentrations. These data indicate a concentration-dependent response of root-tip tissues to BFA. They should not, however, be interpreted as a comprehensive safety assessment. BFA is a biologically active fungal metabolite, and the present experiment should not be regarded as a comprehensive safety assessment. BFA concentrations in medicinal roots and above-ground tissues, transformation products, degradation kinetics, and chronic phytotoxicity were not evaluated. Consumer exposure therefore cannot be assessed from the present data. These issues would need to be resolved before practical application of a BFA-producing strain could be considered.

Antioxidant responses and changes in ginsenoside accumulation

Z1-1031 inoculation was accompanied by marked increases in POD, SOD, and CAT activities in *P. notoginseng* roots. BFA treatment also increased these enzyme activities, particularly during the earlier sampling period, although the responses were less persistent than those observed following fungal inoculation. SOD, POD, and CAT are major components of the enzymatic antioxidant system that contributes to maintenance of cellular redox homeostasis under environmental and biological stress (Barna et al. 2012; Gill and Tuteja 2010). Similar enhancement of antioxidant capacity following inoculation with beneficial fungi has been observed in other plant–microbe systems (Bashir et al. 2026; Hossain et al. 2007; Zheng et al. 2024).

The present results therefore indicate that Z1-1031 and BFA can alter the antioxidant status of *P. notoginseng*. However, increased antioxidant enzyme activity alone does not establish activation of a specific defense-signaling pathway. Previous studies have linked beneficial fungal interactions to jasmonate, salicylate, ROS, and other defense-related signaling processes (Hossain et al. 2007; Zheng et al. 2024). These pathways were not examined in the present study. Consequently, the observed

increases in POD, SOD, and CAT should be interpreted as physiological responses associated with Z1-1031 or BFA treatment, rather than direct evidence for activation of JA-, SA-, or ROS-dependent signaling.

A second physiological response was the transient alteration of ginsenoside accumulation. Z1-1031 significantly increased Rg1 content during the early cultivation period, whereas the difference was no longer significant at the later sampling point. Total measured saponins showed only modest changes. This temporal pattern is noteworthy because it argues against a generalized and sustained enhancement of ginsenoside production. Instead, Z1-1031 appears to have influenced the accumulation of at least one ginsenoside during an early phase of the plant–fungus interaction.

Microbial regulation of secondary metabolism in medicinal plants has been increasingly recognized. Endophytic and rhizospheric microorganisms can be associated with changes in host secondary metabolites, and fungal elicitors have been reported to influence expression of genes involved in ginsenoside biosynthesis (Dang et al. 2021; Ma et al. 2023; Xie et al. 2023; Ye et al. 2021). In *Panax* systems, microbial interactions and nutrient availability can also alter ginsenoside composition (Mu et al. 2024). Recent work further supports a close relationship between Panax rhizosphere processes and regulation of secondary metabolism (Liu 2026).

Nevertheless, the present study did not measure expression of ginsenoside-biosynthetic genes, precursor flux, phytohormones, or nutrient-mediated signaling. The increase in Rg1 therefore cannot presently be assigned to a specific metabolic pathway. The most conservative interpretation is that Z1-1031 inoculation was associated with an early increase in Rg1 accumulation, providing a basis for future investigation of fungal regulation of secondary metabolism in *P. notoginseng*.

Metal biosorption, arsenic transformation, and changes in soil metal concentrations

Z1-1031 also displayed interactions with several metal(loid)s. In laboratory assays, the fungal biomass adsorbed Cd, As, Cu, and Pb, with the greatest biosorption capacity observed for Cd. Fungal cell walls contain multiple metal-binding functional groups, and biosorption by fungal biomass is a well-established physicochemical process contributing to interactions between fungi and environmental metals (Gadd 2010; Mishra et al. 2017). The present data therefore demonstrate an intrinsic metal-binding capacity of Z1-1031, although the relative contribution of this process under cultivation conditions remains to be established.

The arsenic experiment requires a separate interpretation. Z1-1031 caused extensive transformation of As(V) to As(III) in the culture broth, with As(III) becoming the predominant dissolved species at the later sampling point. This demonstrates a strong capacity of Z1-1031 to alter arsenic speciation. However, reduction of As(V) to As(III) should not be interpreted as arsenic detoxification. Arsenic speciation strongly influences its mobility, bioavailability, and toxicity, and As(III) is generally considered more mobile and toxic than As(V). Microbial transformations can therefore either decrease or increase environmental risk depending on the surrounding physicochemical and biological context (Su et al. 2011;

Turpeinen et al. 2002). More broadly, arsenic transformation within the soil–rhizosphere–plant system is complex, and changes in chemical form alone do not demonstrate remediation (Fitz and Wenzel, 2002).

The decrease in total arsenic recovered from the culture system raises an additional question. One possible explanation is microbial volatilization, as proposed for some arsenic-transforming microorganisms. However, volatile arsenic species were not directly collected or quantified in the present study, and a complete arsenic mass balance was not established. The decrease in recoverable arsenic should therefore be described as consistent with an unmeasured loss process, rather than evidence for volatilization.

At both sampling points, Z1-1031-treated cultivation soil showed lower measured concentrations of As, Cd, Pb, and Cu than the corresponding blank controls. The laboratory biosorption results show that Z1-1031 can bind these metals under defined conditions. However, these experiments do not establish fungal biosorption as the cause of the lower metal concentrations observed in cultivation soil. Processes including immobilization, redistribution among soil fractions, leaching, plant uptake, and other microbial transformations were not independently quantified.

This distinction is particularly important for arsenic. Current research shows that microbial and mycorrhizal interactions can substantially alter As speciation, mobility, plant uptake, and antioxidant responses, but evaluating genuine risk reduction requires measurements beyond total soil concentration alone (Hao et al. 2024). Accordingly, the present results support the conclusion that Z1-1031 alters arsenic speciation and is associated with decreases in measured soil metal concentrations, rather than the stronger claim that the strain detoxifies heavy metals or renders *P. notoginseng* safer for medicinal use.

Biological significance and study limitations

Taken together, within the boundaries of the experimental design, Z1-1031 exhibited several experimentally distinguishable activities relevant to *P. notoginseng* cultivation. The strain remained recoverable from rhizosphere soil and was associated with improved plant growth, increased antioxidant enzyme activities, and a transient increase in Rg1. Separately, Z1-1031 produced BFA with *in vitro* antifungal activity, exhibited metal-binding capacity, altered arsenic speciation, and was associated with lower measured soil metal concentrations. These findings are consistent with the broader view that plant-associated microorganisms can influence plant growth, stress responses, secondary metabolism, and rhizosphere chemistry through multiple parallel processes rather than through a single dominant mechanism (Berg et al. 2020; Compant et al. 2021; Trivedi et al. 2020).

Several limitations define the scope of these conclusions. First, although BFA inhibited *F. solani* in vitro and was detected in inoculated rhizosphere soil, no pathogen-challenge experiment was conducted in plants; therefore, in planta biocontrol of root rot has not been demonstrated. Second, CFU recovery demonstrates persistence of Z1-1031 in rhizosphere soil but does not directly demonstrate attachment to root surfaces or colonization of root tissues. Third, the greenhouse experiments comprised three

independent plots per treatment. Although at least ten plants were sampled within each plot at each sampling time to obtain representative plot-level estimates, the number of independent experimental units remained n = 3 per treatment. This limited plot-level sample size reduces statistical power for detecting modest treatment effects and should be considered when interpreting nonsignificant comparisons. Fourth, the signaling pathways underlying the antioxidant and ginsenoside responses were not investigated, and the observed physiological changes therefore cannot be assigned to specific molecular mechanisms. Fifth, although arsenic transformation was demonstrated, volatile arsenic species were not quantified and a complete arsenic mass balance was not established. Arsenic mobility and bioavailable fractions in cultivation soil were also not determined, and metal concentrations and speciation in *P. notoginseng* tissues were not measured. Consequently, the present data cannot establish reduced metal exposure of the medicinal material or reduced environmental risk. Finally, BFA residues in medicinal roots and its broader safety in the plant–soil system were not evaluated; therefore, the safety of applying a BFA-producing strain cannot yet be concluded.

Future studies should first establish in planta efficacy through direct pathogen-challenge experiments and quantify BFA in rhizosphere soil and plant tissues. Additional work should determine the root association of Z1-1031, the mobility, bioavailability, speciation, and plant accumulation of relevant metal(loid)s, and the mass balance of arsenic transformation. These studies will be necessary to determine which of the phenotypes identified here translate into reproducible agronomic benefits and whether Z1-1031 can be considered for practical application in *P. notoginseng* cultivation.

Conclusions

This study demonstrates that *Penicillium janthinellum* Z1-1031 is a *Panax notoginseng*-associated fungus with multiple biological activities relevant to *P. notoginseng* cultivation. Inoculation with Z1-1031 was associated with improved plant survival and growth, increased activities of the antioxidant enzymes SOD, POD, and CAT, and a transient increase in ginsenoside Rg1 content. The strain remained recoverable from rhizosphere soil, where brefeldin A (BFA), identified as a major metabolite of Z1-1031, was detected after inoculation. Purified BFA exhibited concentration-dependent in vitro antifungal activity against *Fusarium solani*. Z1-1031 also showed biosorption capacity toward several metals, transformed As(V) to As(III) under laboratory conditions, and its inoculation was associated with lower measured concentrations of As, Cd, Pb, and Cu in cultivation soil than in the corresponding blank controls. Collectively, these findings characterize Z1-1031 as a plant-associated fungus displaying multiple plant-growth-related, antifungal, antioxidant-response-associated, and metal-interacting phenotypes. However, further studies are required to establish its efficacy against root rot in planta, determine the fate and safety of BFA in the plant–soil system, and clarify the environmental consequences of arsenic transformation and altered soil metal concentrations before practical agricultural application can be considered.

Declarations

Competing interests

The authors have no relevant financial or non-financial interests to disclose.

Ethics declarations

This article does not contain any studies with human participants or animals performed by any of the authors.

Funding

This work was financially supported by the Science and Technology Plan Project of Liaoning Province, People's Republic of China (Grant No. 2025JH5/10400167).

Author Contribution

Conceptualization: Yi-Xuan Zhang; Methodology: Meng-Yue Zhang, Ying-Ying Wu; Formal analysis: Ming Cai, Ping Cao; Investigation: Si-Yu Han, Zheng-Xu Sun, Jun Xie; Data curation: Si-Yu Han; Writing-original draft: Meng-Yue Zhang, Ying-Ying Wu; Writing-review and editing: Yi-Xuan Zhang, Yan-Jun Hao.

Data availability

The datasets generated and/or analyzed during the current study are available from the corresponding author upon reasonable request.

References

1. Akram S, Ahmed A, He P, He P, Liu Y, Wu Y, Munir S, He Y (2023) Uniting the role of endophytic fungi against plant pathogens and their interaction. J Fungi 9:72. https://doi.org/10.3390/jof9010072
2. Avis TJ, Gravel V, Antoun H, Tweddell RJ (2008) Multifaceted beneficial effects of rhizosphere microorganisms on plant health and productivity. Soil Biol Biochem 40:1733–1740. https://doi.org/10.1016/j.soilbio.2008.02.013
3. Barna B, Fodor J, Harrach BD, Pogány M, Király Z (2012) The Janus face of reactive oxygen species in resistance and susceptibility of plants to necrotrophic and biotrophic pathogens. Plant Physiol Biochem 59:37–43. https://doi.org/10.1016/j.plaphy.2012.01.014
4. Baron NC, Rigobelo EC (2022) Endophytic fungi: a tool for plant growth promotion and sustainable agriculture. Mycology 13:39–55. https://doi.org/10.1080/21501203.2021.1945699

5. Bashir T, Haq SAU, Husaini AM (2026) Organic priming strategies enhance antioxidant defense and suppress corm rot in saffron: role of *Trichoderma* and walnut leaf powder. Protoplasma 263:1301–1314. https://doi.org/10.1007/s00709-026-02170-5
6. Berg G, Rybakova D, Fischer D, Cernava T, Vergès MC, Charles T, Chen X, Cocolin L, Eversole K, Corral GH, Kazou M, Kinkel L, Lange L, Lima N, Loy A, Macklin JA, Maguin E, Mauchline T, McClure R, Mitter B, Ryan M, Sarand I, Smidt H, Schelkle B, Roume H, Kiran GS, Selvin J, Souza RSC, van Overbeek L, Singh BK, Wagner M, Walsh A, Sessitsch A, Schloter M (2020) Microbiome definition re-visited: old concepts and new challenges. Microbiome 8:103. https://doi.org/10.1186/s40168-020-00875-0
7. Chen J, Liu Z, Liu Y, Ji X, Li X, Wei Y, Zi F, Tan Y (2024) Differences in autotoxic substances and microbial community in the root space of *Panax notoginseng* coinducing the occurrence of root rot. Appl Environ Microbiol 90:e02287–e02223. https://doi.org/10.1128/aem.02287-23
8. Compant S, Cambon MC, Vacher C, Mitter B, Samad A, Sessitsch A (2021) The plant endosphere world—bacterial life within plants. Environ Microbiol 23:1812–1829. https://doi.org/10.1111/1462-2920.15240
9. Dang H, Zhang T, Wang Z, Li G, Zhao W, Lv X, Zhuang L (2021) Succession of endophytic fungi and arbuscular mycorrhizal fungi associated with the growth of plant and their correlation with secondary metabolites in the roots of plants. BMC Plant Biol 21:165. https://doi.org/10.1186/s12870-021-02942-6
10. Dasila K, Pandey A, Sharma A, Samant SS, Singh M (2024) Endophytic fungi from Himalayan silver birch as potential source of plant growth enhancement and secondary metabolite production. Braz J Microbiol 55:557–570. https://doi.org/10.1007/s42770-024-01259-4
11. Dong TT, Cui XM, Song ZH, Zhao KJ, Ji ZN, Lo CK, Tsim KW (2003) Chemical assessment of roots of *Panax notoginseng* in China: regional and seasonal variations in its active constituents. J Agric Food Chem 51:4617–4623. https://doi.org/10.1021/jf034229k
12. Fan T, Liu Y, Feng B, Zeng G, Yang C, Zhou M, Zhou H, Tan Z, Wang X (2008) Biosorption of cadmium(II), zinc(II) and lead(II) by *Penicillium simplicissimum*: isotherms, kinetics and thermodynamics. J Hazard Mater 160:655–661. https://doi.org/10.1016/j.jhazmat.2008.03.038
13. Fitz WJ, Wenzel WW (2002) Arsenic transformations in the soil–rhizosphere–plant system: fundamentals and potential application to phytoremediation. J Biotechnol 99:259–278. https://doi.org/10.1016/S0168-1656(02)00218-3
14. Gadd GM (2010) Metals, minerals and microbes: geomicrobiology and bioremediation. Microbiology 156:609–643. https://doi.org/10.1099/mic.0.037143-0
15. Gill SS, Tuteja N (2010) Reactive oxygen species and antioxidant machinery in abiotic stress tolerance in crop plants. Plant Physiol Biochem 48:909–930. https://doi.org/10.1016/j.plaphy.2010.08.016
16. Hao S, Tian Y, Lin Z, Xie L, Zhou X, Bañuelos GS (2024) Effects of arbuscular mycorrhizal fungi on the reduction of arsenic accumulation in plants: a meta-analysis. Front Plant Sci 15:1327649. https://doi.org/10.3389/fpls.2024.1327649

17. Hossain MM, Sultana F, Kubota M, Koyama H, Hyakumachi M (2007) The plant growth-promoting fungus *Penicillium simplicissimum* GP17-2 induces resistance in *Arabidopsis thaliana* by activation of multiple defense signals. Plant Cell Physiol 48:1724–1736. https://doi.org/10.1093/pcp/pcm144
18. Jayaraman S, Naorem AK, Lal R, Dalal RC, Sinha NK, Patra AK, Chaudhari SK (2021) Disease-suppressive soils—beyond food production: a critical review. J Soil Sci Plant Nutr 21:1437–1465. https://doi.org/10.1007/s42729-021-00451-x
19. Khan SA, Hamayun M, Yoon H, Kim HY, Suh SJ, Hwang SK, Kim JM, Lee IJ, Choo YS, Yoon UH, Kong WS, Lee BM, Kim JG (2008) Plant growth promotion and *Penicillium citrinum*. BMC Microbiol 8:231. https://doi.org/10.1186/1471-2180-8-231
20. Liu L, Wang Z, Luo C, Deng Y, Wu W, Jin Y, Wang Y, Huang H, Wei Z, Zhu Y, He X, Guo L (2025a) Beneficial soil microbiome profiles assembled using tetramycin to alleviate root rot disease in *Panax notoginseng*. Front Microbiol 16:1571684. https://doi.org/10.3389/fmicb.2025.1571684
21. Liu M, Du X, Wang M, Huo Y, Zeng Y, Wu J, Ying X, Wei F, Liu L, Tang J (2025b) The hormesis effect of cadmium on *Panax notoginseng* and corresponding impact on the rhizosphere microorganism. Ecotoxicol Environ Saf 291:117839. https://doi.org/10.1016/j.ecoenv.2025.117839
22. Liu P (2026) Advances in rhizosphere microbiome research of *Panax* species: structure and function, interactions, and applications. Rhizosphere 38:101329. https://doi.org/10.1016/j.rhisph.2026.101329
23. Lugtenberg B, Kamilova F (2009) Plant-growth-promoting rhizobacteria. Annu Rev Microbiol 63:541–556. https://doi.org/10.1146/annurev.micro.62.081307.162918
24. Ma L, Cao YH, Cheng MH, Huang Y, Mo MH, Wang Y, Yang JZ, Yang FX (2013) Phylogenetic diversity of bacterial endophytes of *Panax notoginseng* with antagonistic characteristics towards pathogens of root-rot disease complex. Antonie Van Leeuwenhoek 103:299–312. https://doi.org/10.1007/s10482-012-9810-3
25. Ma N, Yin D, Liu Y, Gao Z, Cao Y, Chen T, Huang Z, Jia Q, Wang D (2023) Succession of endophytic fungi and rhizosphere soil fungi and their correlation with secondary metabolites in *Fagopyrum dibotrys*. Front Microbiol 14:1220431. https://doi.org/10.3389/fmicb.2023.1220431
26. Matsukuma S, Nishizuka Y, Watanabe J, Okuda T (1994) Identification of *Penicillium* sp. NR 6564 and taxonomic notes on *P. janthinellum*. Mycoscience 35:183–186. https://doi.org/10.1007/BF02318498
27. Miao ZQ, Li SD, Liu XZ, Chen YJ, Li YH, Wang Y, Guo RJ, Xia ZY, Zhang KQ (2006) The causal microorganisms of *Panax notoginseng* root rot disease. Sci Agric Sin 39:1371–1378. https://doi.org/10.3321/j.issn:0578-1752.2006.07.011
28. Mishra J, Singh R, Arora NK (2017) Alleviation of heavy metal stress in plants and remediation of soil by rhizosphere microorganisms. Front Microbiol 8:1706. https://doi.org/10.3389/fmicb.2017.01706
29. Mu P, Ding G, Zhang Y, Jin Q, Liu Z, Guan Y, Zhang L, Liang C, Zhou F, Liu N (2024) Interactions between arbuscular mycorrhizal fungi and phosphate-soluble bacteria affect ginsenoside

compositions by modulating the C:N:P stoichiometry in *Panax ginseng*. Front Microbiol 15:1426440. https://doi.org/10.3389/fmicb.2024.1426440

30. Narendrula-Kotha R, Nkongolo KK (2017) Microbial response to soil liming of damaged ecosystems revealed by pyrosequencing and phospholipid fatty acid analyses. PLoS ONE 12:e0168497. https://doi.org/10.1371/journal.pone.0168497
31. Ou X, Wang L, Guo L, Cui X, Liu D, Yang Y (2016) Soil-plant metal relations in *Panax notoginseng*: an ecosystem health risk assessment. Int J Environ Res Public Health 13:1089. https://doi.org/10.3390/ijerph13111089
32. Prasad A, Patel P, Niranjan A, Mishra A, Saxena G, Singh SS, Chakrabarty D (2022) Biotic elicitor-induced changes in growth, antioxidative defense, and metabolites in an improved prickleless *Solanum viarum*. Appl Microbiol Biotechnol 106:6455–6469. https://doi.org/10.1007/s00253-022-12159-8
33. Qin X, Xu J, An X, Yang J, Wang Y, Dou M, Wang M, Huang J, Fu Y (2024) Insight of endophytic fungi promoting the growth and development of woody plants. Crit Rev Biotechnol 44:78–99. https://doi.org/10.1080/07388551.2022.2129579
34. Rasool S, Groos M, Hannula SE, Biere A (2025) Bioinoculant-induced plant resistance is modulated by interactions with resident soil microbes. Environ Microbiome 20:7. https://doi.org/10.1186/s40793-025-00667-9
35. Razzaq A, Zafar MM, Ali A, Ihsan L, Qadir F, Khan MN, Zhang Y, Gao L, Cong H, Iqbal R, Jiang X, Qiao F (2025) Elicitor-mediated enhancement of secondary metabolites in plant species: a review. Front Plant Sci 16:1706600. https://doi.org/10.3389/fpls.2025.1706600
36. Su S, Zeng X, Bai L, Li L, Duan R (2011) Arsenic biotransformation by arsenic-resistant fungi *Trichoderma asperellum* SM-12F1, *Penicillium janthinellum* SM-12F4, and *Fusarium oxysporum* CZ-8F1. Sci Total Environ 409:5057–5062. https://doi.org/10.1016/j.scitotenv.2011.08.039
37. Sun HX, Qin F, Ye YP (2005) Relationship between haemolytic and adjuvant activity and structure of protopanaxadiol-type saponins from the roots of *Panax notoginseng*. Vaccine 23:5533–5542. https://doi.org/10.1016/j.vaccine.2005.07.036
38. Tan Y, Cui Y, Li H, Kuang A, Li X, Wei Y, Ji X (2017) Diversity and composition of rhizospheric soil and root endogenous bacteria in *Panax notoginseng* during continuous cropping practices. J Basic Microbiol 57:337–344. https://doi.org/10.1002/jobm.201600464
39. Thuerig B, Binder A, Boller T, Guyer U, Jiménez S, Rentsch C, Tamm L (2006) An aqueous extract of the dry mycelium of *Penicillium chrysogenum* induces resistance in several crops under controlled and field conditions. Eur J Plant Pathol 114:185–197. https://doi.org/10.1007/s10658-005-4512-6
40. Trivedi P, Leach JE, Tringe SG, Sa T, Singh BK (2020) Plant–microbiome interactions: from community assembly to plant health. Nat Rev Microbiol 18:607–621. https://doi.org/10.1038/s41579-020-0412-1
41. Turpeinen R, Kairesalo T, Pantsar-Kallio M (2002) Role of microbes in controlling the speciation of arsenic and production of arsines in contaminated soils. Sci Total Environ 285:133–145.

https://doi.org/10.1016/S0048-9697(01)00903-2

42. Valix M, Tang JY, Malik R (2001) Heavy metal tolerance of fungi. Min Eng 14:499–505. https://doi.org/10.1016/S0892-6875(01)00037-1
43. Viterbo A, Landau U, Kim S, Chernin L, Chet I (2010) Characterization of ACC deaminase from the biocontrol and plant growth-promoting agent *Trichoderma asperellum* T203. FEMS Microbiol Lett 305:42–48. https://doi.org/10.1111/j.1574-6968.2010.01910.x
44. Wang FW, Jiao RH, Cheng AB, Tan SH, Song YC (2007) Antimicrobial potentials of endophytic fungi residing in *Quercus variabilis* and brefeldin A obtained from *Cladosporium* sp. World J Microbiol Biotechnol 23:79–83. https://doi.org/10.1007/s11274-006-9195-4
45. Wang WY, Zhao CL, Chen ZJ, Wen GS, Wei FG, Long TJ, Li SW, Wang CD (2015) Studies on the isolation, identification and in vitro growth rates of the three pathogenic fungi from *Panax notoginseng* cultivated in Wenshan eparchy. Agric Sci Technol 16:1165–1171
46. Wen J, Okyere SK, Wang S, Wang J, Xie L, Ran Y, Hu Y (2022) Endophytic fungi: an effective alternative source of plant-derived bioactive compounds for pharmacological studies. J Fungi 8:205. https://doi.org/10.3390/jof8020205
47. Wu W, Wan X, Shah F, Fahad S, Huang J (2014) The role of antioxidant enzymes in adaptive responses to sheath blight infestation under different fertilization rates and hill densities. ScientificWorldJournal 2014:502134. https://doi.org/10.1155/2014/502134
48. Xie J, Wu YY, Zhang TY, Zhang MY, Zhu WW, Gullen EA, Wang ZJ, Cheng YC, Zhang YX (2017) New and bioactive natural products from an endophyte of *Panax notoginseng*. RSC Adv 7:38100–38109. https://doi.org/10.1039/C7RA07060H
49. Xie J, Wu YY, Zhang TY, Zhang MY, Peng F, Lin B, Zhang YX (2018) New antimicrobial compounds produced by endophytic *Penicillium janthinellum* isolated from *Panax notoginseng* as potential inhibitors of FtsZ. Fitoterapia 131:35–43. https://doi.org/10.1016/j.fitote.2018.10.006
50. Xie XG, Zhang ZZ, Chen L, Ming QL, Sheng KX, Chen X, Rahman K, Feng KM, Su J, Han T (2023) An endophytic fungus *Schizophyllum commune* isolated from *Panax ginseng* enhances hairy roots growth and ginsenoside biosynthesis. Can J Microbiol 69:296–308. https://doi.org/10.1139/cjm-2022-0194
51. Yan XL, Liao XY, Yu BB, Zhang WB (2011) Accumulation of soil arsenic by *Panax notoginseng* and its associated health risk. Huan Jing Ke Xue 32:880–885
52. Ye HT, Luo SQ, Yang ZN, Wang YS, Ding Q, Wang KF, Yang SX, Wang Y (2021) Endophytic fungi stimulate the concentration of medicinal secondary metabolites in *Houttuynia cordata* Thunb. Plant Signal Behav 16:1929731. https://doi.org/10.1080/15592324.2021.1929731
53. Zheng F, Fu Y, Yu P, Qin C, Guo T, Xu H, Chen J, Ahammed GJ, Liu A, Chen S (2024) Flavonoid synthesis is crucial for *Trichoderma asperellum*-induced systemic resistance to root-knot nematodes in tomato plants. Plant Physiol Biochem 212:108706. https://doi.org/10.1016/j.plaphy.2024.108706

Figures

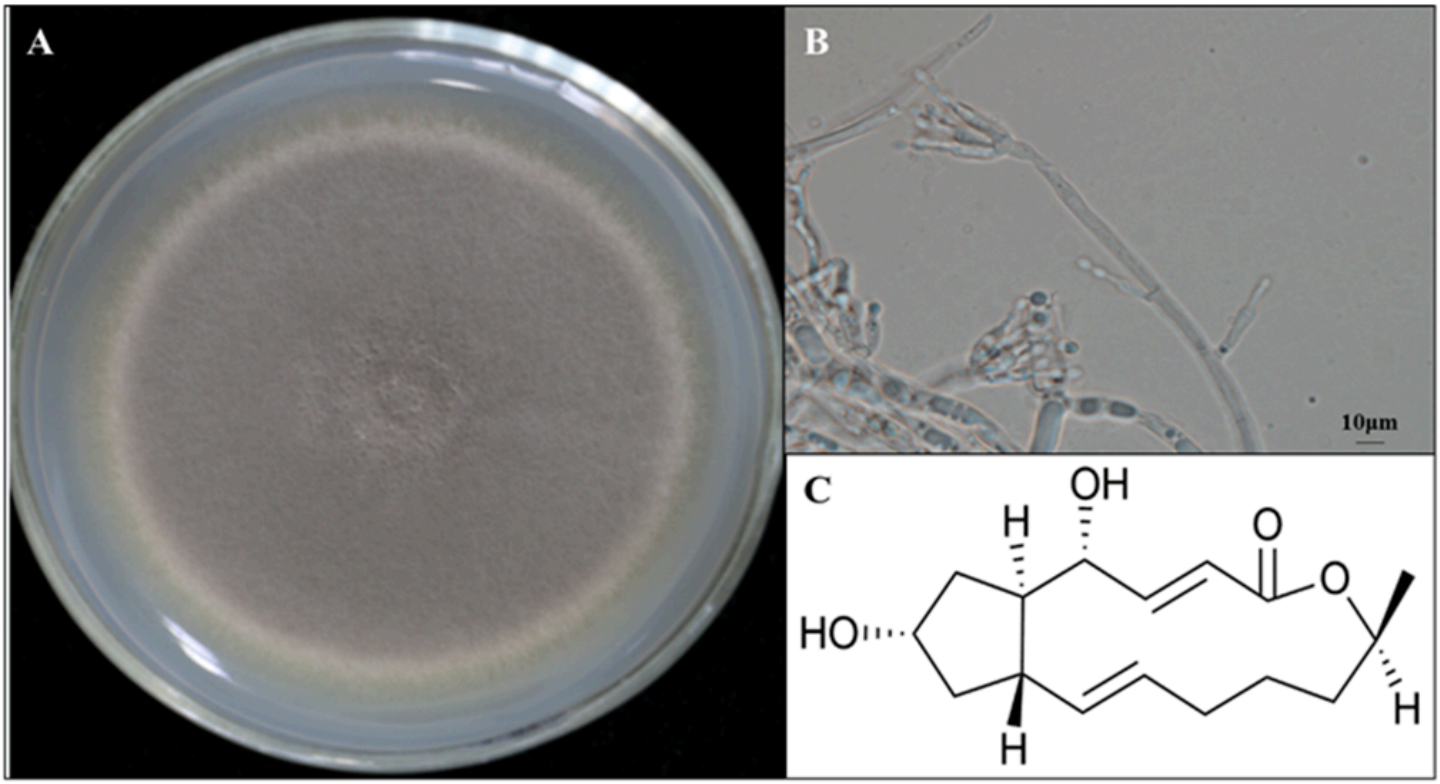


Figure 1

Morphological images of *P. janthinellum* Z1-1031 and chemical structure of metabolite BFA. (A) colony on PDA; (B) conidia ×100; (C) chemical structure of BFA.

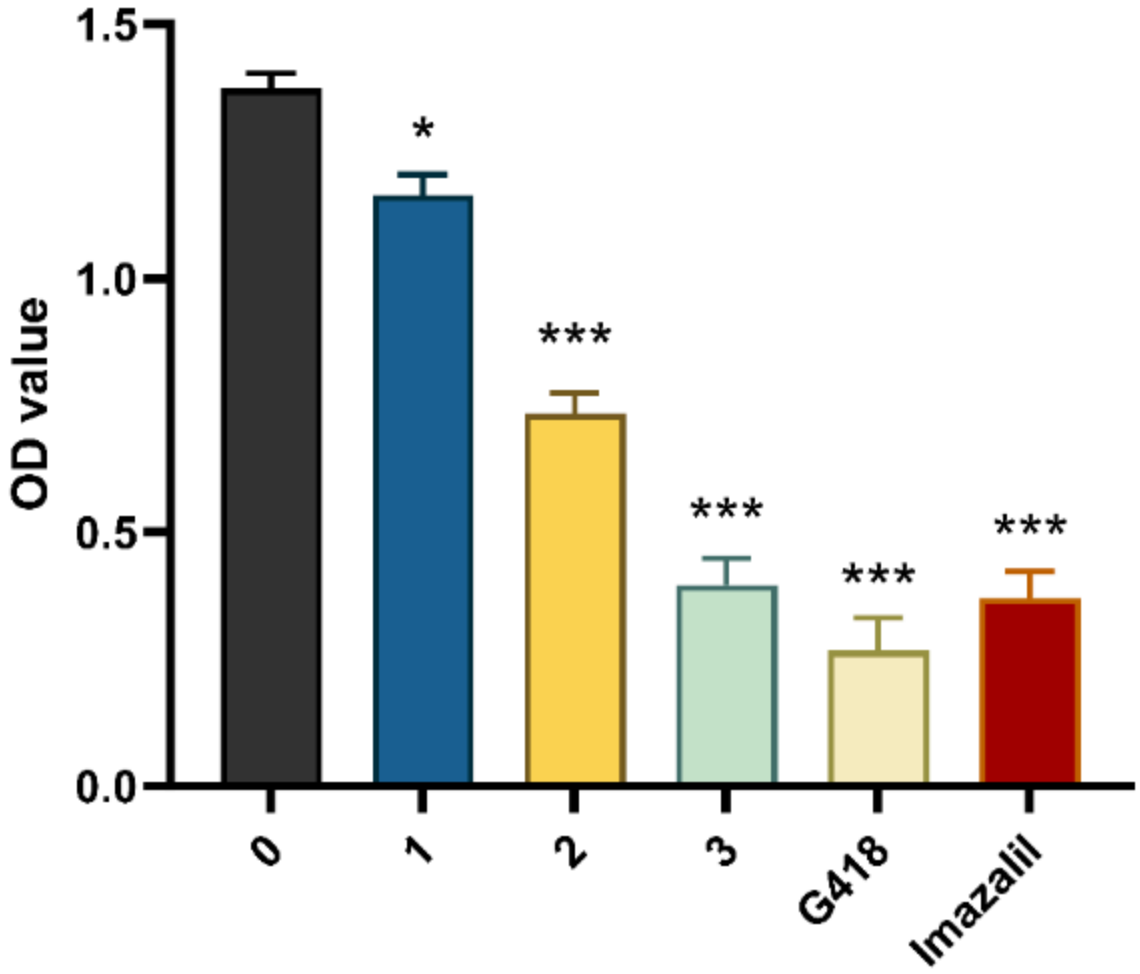


Figure 2

In vitro antifungal activity of brefeldin A (BFA) against *Fusarium solani*. Fungal growth was evaluated by measuring OD values after treatment with different concentrations of BFA: (0) 0, (1) 20, (2) 200, and (3) 1000 μg mL^{-1}. G418 (2 μg mL^{-1}) and Imazalil (2 μg mL^{-1}) were used as positive controls. Data are presented as mean ± standard deviation (SD) from three independent experiments. Statistical significance between the control and treatment groups was analyzed using one-way ANOVA followed by Tukey's multiple comparison test (*$P < 0.05$, **$P < 0.01$, ***P < 0.001).

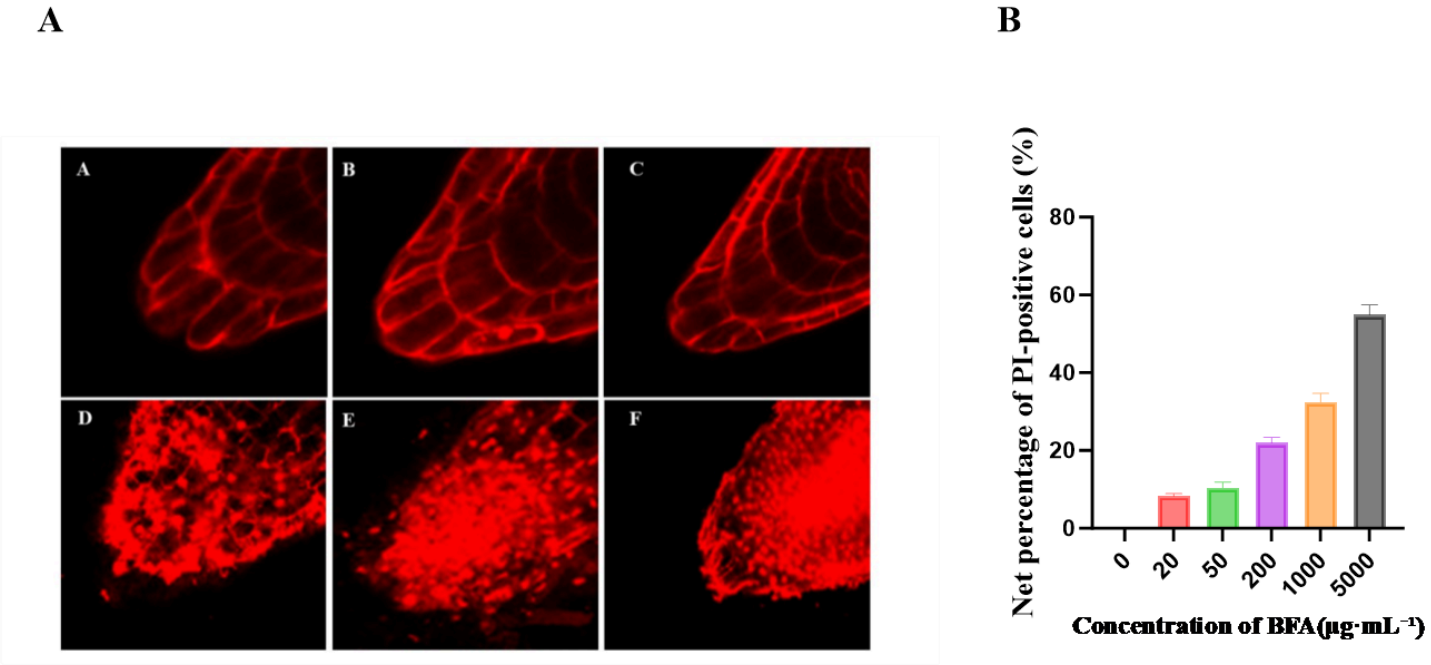


Figure 3

Effects of BFA on membrane integrity of *Panax notoginseng* root-tip cells as assessed by propidium iodide (PI) staining. (A) Representative PI staining images of *P. notoginseng* apical root cells after treatment with different concentrations of BFA: (a) 0 μg·mL⁻¹ (control), (b) 20 μg·mL⁻¹, (c) 50 μg·mL⁻¹, (d) 200 μg·mL⁻¹, (e) 1000 μg·mL⁻¹, (f) 5000 μg·mL⁻¹. Red fluorescence indicates PI-positive cells with damaged plasma membranes. (B) Quantitative analysis of PI-positive cells in *P. notoginseng* root tips under different BFA concentrations. The percentage of PI-positive cells was quantified using ImageJ by calculating the ratio of red fluorescence area to the total root tip area. Data are presented as mean ± SD of three independent biological replicates (n = 3). Differences among BFA concentrations were analyzed by one-way ANOVA followed by Tukey's multiple-comparison test.

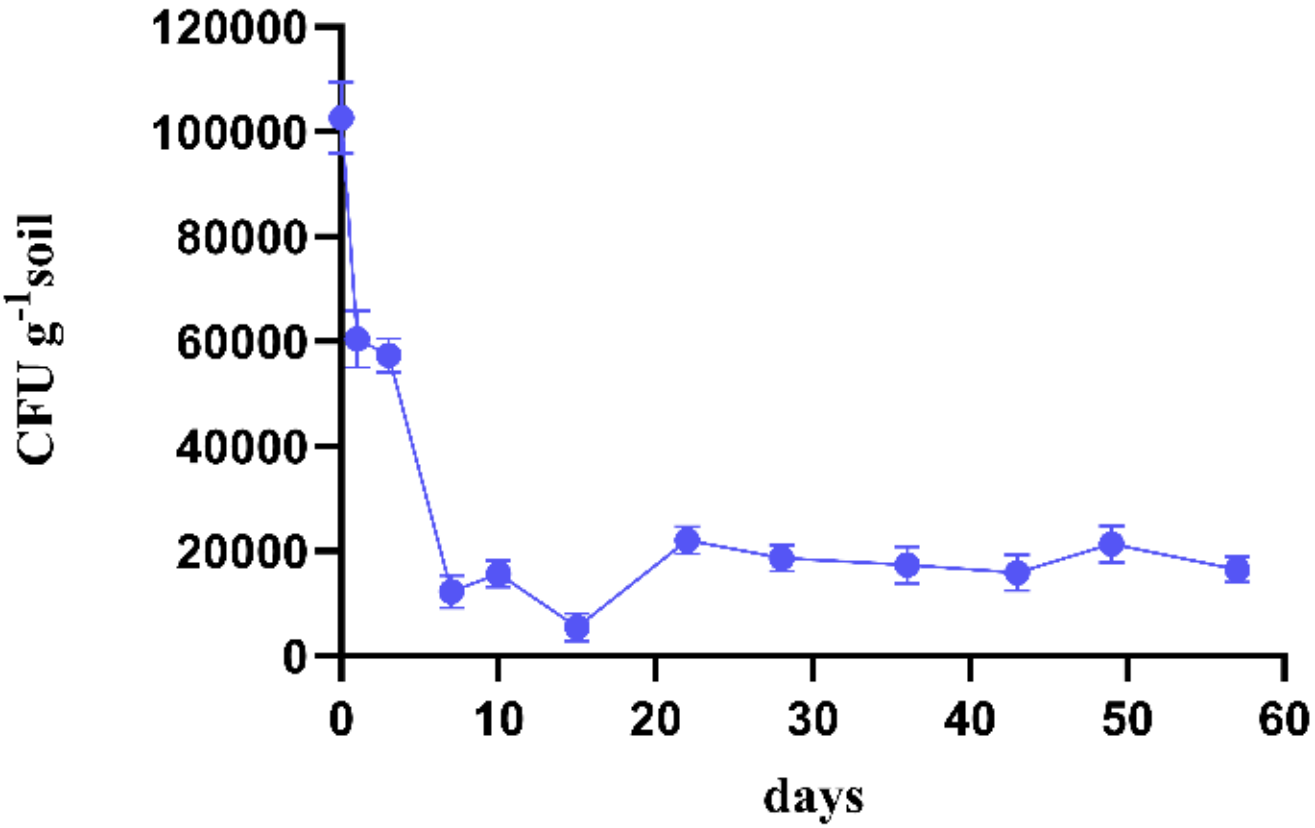


Figure 4

Survival dynamics of strain Z1-1031-egfp in rhizosphere soil after inoculation. Colony-forming units (CFU g⁻¹ soil) were quantified at the indicated time points to monitor persistence of the EGFP-labelled strain. Data are presented as mean ± SD of three independent experiments.

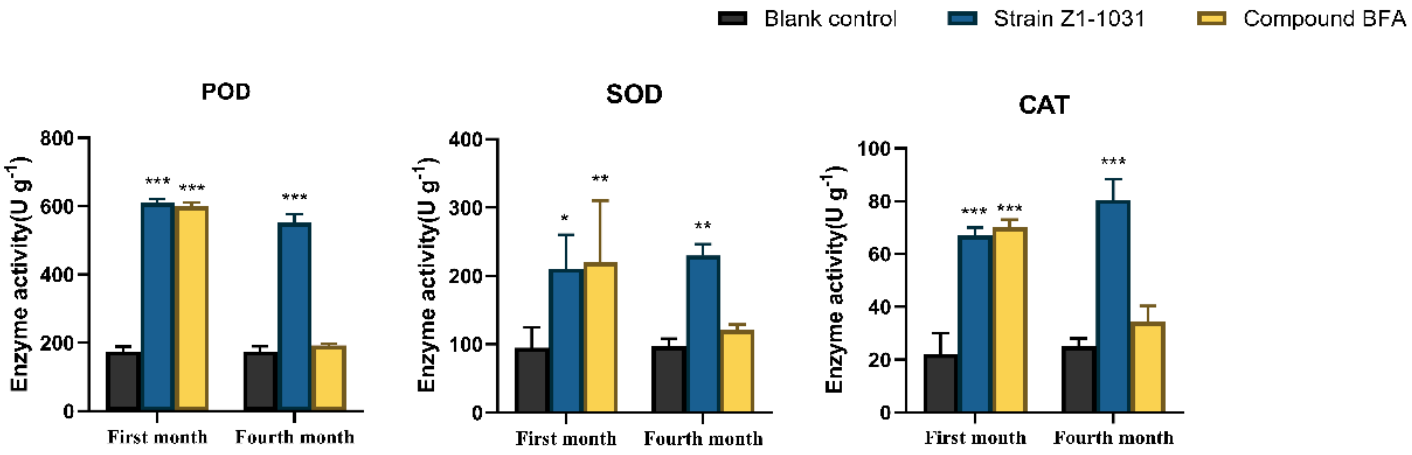


Figure 5

Effects of strain Z1-1031 and brefeldin A (BFA) on antioxidant enzyme activities in roots of Panax notoginseng. Activities of peroxidase (POD), superoxide dismutase (SOD), and catalase (CAT) were measured after one and four months of treatment. Data are presented as mean ± standard deviation (SD) of three independent plots (n = 3). For each enzyme, treatment, time, and the treatment × time interaction were analyzed using a linear mixed-effects model with plot nested within treatment as a random effect. Pairwise comparisons among treatments at each sampling time were adjusted using Tukey's method. Asterisks indicate significant differences from the corresponding blank control at the same sampling time (*P < 0.05, **P < 0.01, ***P < 0.001).

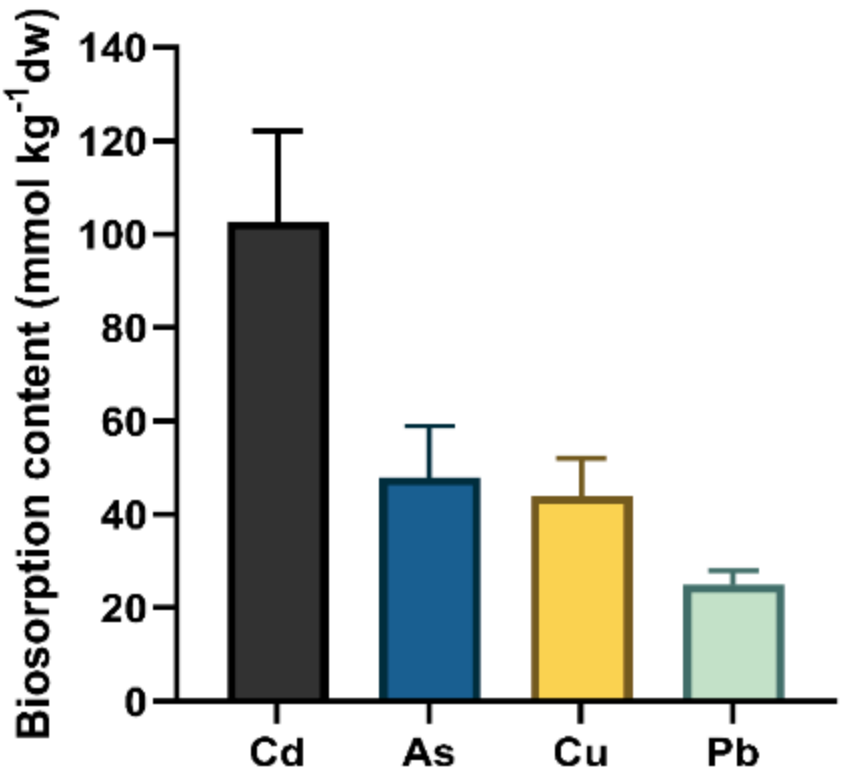


Figure 6

Biosorption capacity of strain Z1-1031 toward different heavy metals. The biosorption of Cd, As, Cu, and Pb by strain Z1-1031 was determined after incubation with fungal biomass. Biosorption capacity is expressed as mmol kg^{-1} dry weight (dw). Data are presented as mean ± SD of three independent culture experiments (n = 3).

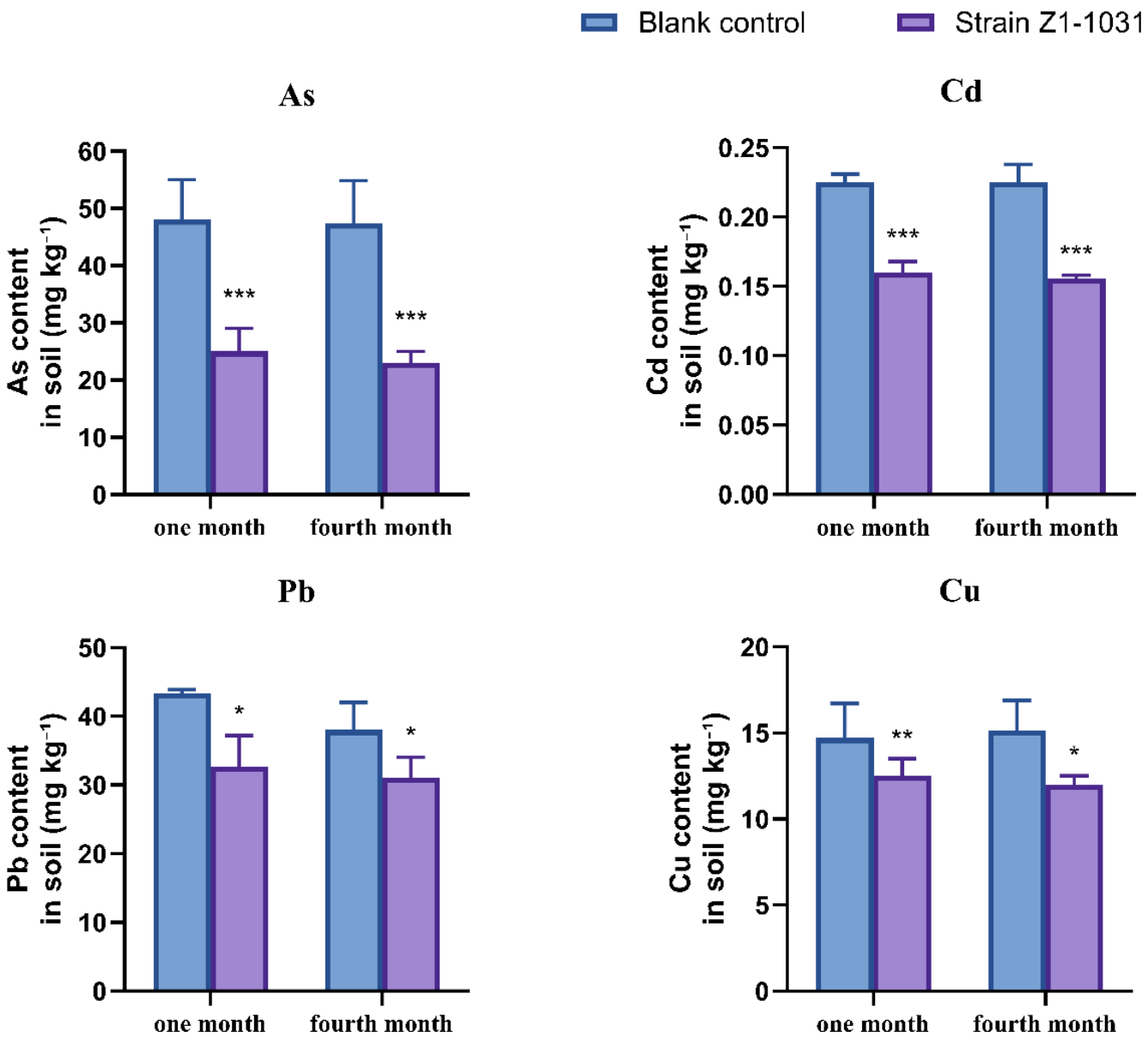


Figure 7

Changes in soil metal concentrations following treatment with strain Z1-1031. Concentrations of arsenic (As), cadmium (Cd), lead (Pb), and copper (Cu) were determined in blank-control and Z1-1031-treated cultivation soils after one and four months. Metal concentrations are expressed as mg kg^{-1} dry soil. Data are presented as mean ± standard deviation (SD) of three independent plots (n = 3). For each metal, treatment, time, and the treatment × time interaction were analyzed using a linear mixed-effects model with plot nested within treatment as a random effect. Pairwise comparisons between the blank control and Z1-1031 treatment at each sampling time were adjusted for multiple comparisons. Asterisks indicate significant differences at the sampling time (*$P < 0.05$, **$P < 0.01$, ***$P < 0.001$).

Supplementary Files

This is a list of supplementary files associated with this preprint. Click to download.

- ManuscriptV25SupplementaryInformation.pdf